Journal of Innovative Technology, Vol. 2, No. 2, pp. 53-60, September 2020
http://doi.org/10.29424/JIT.202009_2(2).0009

Sensing Characteristics of a Chloride Sensor Utilizing the XBee Wireless Sensing System

Shi-Chang Tseng [1], Tong-Yu Wu [2], Jung-Chuan Chou [3*], Po-Yu Kuo [4], Chih-Hsien Lai [5], Yu-Hsun Nien [6], Yi-Hung Liao [7], Si-Hong Lin [8], and Tsu-Yang Lai [9]

ABSTRACT

Water quality monitoring becomes vital as nations industrialize and centrally plan utilities. This paper examines the sensing characteristics of a flexible arrayed chloride sensor combined with an XBee wireless sensing system. The average sensitivity of the wireless chloride sensing device was 47.84 mV/pCl and linearity was 0.99. The hysteresis voltages were 50.14 mV and 36.71 mV during different solution cycles, with one solution cycle being 1 M → 10^{-1} M → 1 M → 10^{-3} M → 1 M, and the alternate being 1 M → 10^{-3} M → 1 M → 10^{-1} M → 1 M. Interference experiments were conducted to obtain selectivity coefficients for the ClO^- ion, ClO_4^- ion, NO_3^- ion and I^- ion for Cl^- ion, which were 5.0×10^{-2}, 1.0×10^{-1}, 5.9×10^{-3} and 5.6×10^{-1}, respectively. Sensing characteristics for real-time wireless measurement were tested using a dynamic microfluidic system. The sensitivity was 60.64 mV/pCl and linearity was 0.98 at 35 μL/min.

Keywords: Flexible arrayed chloride sensor, XBee wireless sensing system, Hysteresis voltage, Selectivity coefficient, Dynamic microfluidic.

1. INTRODUCTION

Industrialized nations frequently face common issues with regard to water pollution. Accordingly, monitoring water quality is becoming an increasingly important consideration as more nations reach this stage of development. A number of researchers (Aisopou, Stoianov and Graham, 2012; Carbó *et al*. 2018; Gonski *et al*. 2018; Kato *et al*. 2017;) have used chemical or optical sensors to measure and analyze water composition and quality. Gonski and colleagues (2018) used a Honeywell Durafet pH sensor to measure pH variation in rivers. Kato and colleagues (2017) investigated residual chloride concentrations in tap water through the use of compensating electrodes; and they also successfully calibrated residual chloride selectivity for their sensors using hydrogen ion concentration (pH) and dissolved oxygen (DO). Aisopou and colleagues (2012) used electrochemical and optical technologies to measure a number of water aspects including electrical conductivity, pH, free chloride, total chloride, DO, oxidative redox potential (ORP) and turbidity. Carbó and colleagues (2018) used a voltammetric electronic tongue and pulse method to investigate the characteristics of spring water. The pH ranges of the spring water samples ranged from 7.3 to 7.8. The trace chemical compositions of the samples included chloride, nitrate, sodium, sulfate and fluoride.

Li and colleagues (2017) used black phosphorus (BP) to prepare a chemical sensor. Rapid, label-free trace detection of mercury Hg^{2+} was achieved with detection limit of 0.01 ppb, lower than the world health organization (WHO) tolerance level (1 ppb). Later, Li and colleagues (2018) again used BP to prepare a flexible integrated BP chemical sensor array (FIBA). The FIBA was able to sense Hg^{2+} ions, cadmium (Cd^{2+}) ions, lead (Pb^{2+}) ions and sodium (Na^+) ions. The detection limit for Hg^{2+} ions remained at 0.01 ppb.

Drawbacks in water quality monitoring research to date relate to limitations in detection distance and operational space. Thus, many researchers instead elected to research different ion detection methods and record experimental their findings using wireless sensing systems (Abbas *et al*. 2015; Cheng *et al*. 2012; Chou, Chen, and Lee 2012; Croce *et al*. 2015; Dam, Zevenbergen, and Schaijk, 2016; Dang et al. 2018; Harris *et al*. 2016; Jung *et al*. 2017; Lu *et al*. 2015; Nyni *et al*. 2017; Ong, Paulose, and Grimes, 2003; Rahimi *et al*. 2018; Smettem *et al*. 2017; Yue, and Ying, 2012; Zhou *et al*. 2015; Zhou *et al*. 2017; Zhuiykov, 2012).

Zhuiykov (2012) investigated wireless sensing devices to measure electrical conductivity, pH, dissolved metal ions, dissolved oxygen (DO) and dissolved organic carbon (DOC). Ong

Manuscript received August 3, 2020; revised August 19, 2020; accepted August 27, 2020.

[1] Professor, Department of Mechanical Engineering, National Yunlin University of Science and Technology, Douliou, Taiwan 64002, R.O.C.
[2] Graduate Student, Department of Mechanical Engineering, National Yunlin University of Science and Technology, Douliou, Taiwan 64002, R.O.C.
[3*] Chair Professor (corresponding author), Department of Electronic Engineering, National Yunlin University of Science and Technology, Douliou, Yunlin, Taiwan 64002, R.O.C. (e-mail: choujc@yuntech.edu.tw).
[4] Assistant Professor, Department of Electronic Engineering, National Yunlin University of Science and Technology, Douliou, Yunlin, Taiwan 64002, R.O.C.
[5] Professor, Department of Electronic Engineering, National Yunlin University of Science and Technology, Douliou, Yunlin, Taiwan 64002, R.O.C.
[6] Professor, Department of Chemical and Materials Engineering, National Yunlin University of Science and Technology, Douliou, Yunlin, Taiwan 64002, R.O.C.
[7] Professor, Department of Information and Electronic Commerce Management, TransWorld University, Yunlin, Taiwan 64002, R.O.C.
[8] Graduate Student, Department of Electronic Engineering, National Yunlin University of Science and Technology, Douliou, Yunlin, Taiwan 64002, R.O.C.
[9] Postgraduate, Department of Electronic Engineering, National Yunlin University of Science and Technology, Douliou, Yunlin, Taiwan 64002, R.O.C.

and colleagues (2003) accurately detected hypochlorite ion variations using a wireless sensing device. Their hypochlorite ion sensor consisted of a layer of polyurethane and alumina on a magnetically-soft ferromagnetic ribbon. Zhou and colleagues (2017) used a Ag/AgCl electrode, reference electrode, and the radio-frequency identification (RFID) communication protocol to measure and investigate chloride ion concentrations in concrete. Harris and colleagues (2016) used screen printing technology to develop a low-cost, robust chloride ion sensor and proceeded to investigate the sensor characteristics using the IEEE 802.15.4 standard wireless personal area network protocols, while recording data to a secure digital (SD) memory card. Chloride sensors were applied to measure the chloride ion concentration for soil columns, fluvarium and greenhouses. Nyni and colleagues (2017) developed wireless health monitoring systems for humans, which included an electro cardio gram (ECG), electroencephalogram (EEG) and electromyogram (EMG). They used an arduino UNO board and Bluetooth module to construct their wireless transmission system. Cheng and colleagues (2012) fabricated a chloride ion sensing device and a Bluetooth wireless measurement system. The wireless sensing devices were used to obtain response voltages from 10^{-4} M to 1 M NaCl solutions.

The current-voltage (I-V) measurement system was integrated with three Keithley 236 semiconductor parameter analyzers (Chou, Chen, and Lee, 2012). Dam and colleagues (2016) prepared a sweat sensing device by screen printing, integrating the sensing device with a high impedance voltmeter (Keithley 617A, Keithley Instruments Company, U.S.A.). Hysteresis effects and detected chloride ion concentrations were all recorded. Smettem and colleagues (2017) prepared and integrated wireless chloride ion sensing devices using screen printing techniques, a central microcontroller (MCU), real-time clocks (RTC), a GPS module and the IEEE 802.15.4 standard. Their wireless chloride ion sensing devices have since been used to monitor the water quality of streams. Abbas and colleagues (2015) investigated the sensing characteristics of near-field-inductive coupling (NFC) of sensing devices and readout coils with Ag/AgCl electrodes. Capacitance variations ranged from 180 pF to 200 pF when chloride ion concentrations ranged between 0.01 M and 0.2 M, respectively. Jung and colleagues (2017) used a three-electrode electrochemical amperometric analyzer to investigate sensing characteristics on a range of 1 mM to 100 mM of ruthenium chloride. Three electrodes, a current-to-voltage (I/V) measurement system, a Bluetooth 4.0 module (WT-12, Bluegiga, Espoo, Finland) and a notebook computer were used to set up a three-electrode electrochemical amperometric analyzer. They prepared a silver (Ag) counter electrode and silver-silver chloride (Ag/AgCl) reference electrode and an indium tin oxide (ITO) working electrode on ITO glass.

Yue and Ying (2012) integrated a solar power supply with a wireless sensor system. The wireless sensors were used to detect pH, turbidity and oxygen density. Dang and colleagues (2018) used a graphite-polyurethane composite to prepare a pH sensor where the RFID pH sensor was used to detect sweat pH variations; average sensitivity was found to be 11.13 mV/pH. Lu and colleagues (2015) investigated human gastrointestinal (GI) physiological information by wireless capsule. They prepared a pH micro sensor, pressure micro sensor, temperature micro sensor and radio frequency (RF) transceiver in a wireless capsule. The wireless capsule was tested on living animals (pigs in this case) and three healthy volunteers. They obtained data related to pH, temperature and pressure from the capsule.

Rahimi and colleagues (2018) prepared a transparent pH sensor and NFC wireless measurements for the monitoring of wound infections. The transparent wireless NFC pH sensor was also used to investigate hysteresis effects and drift effects in the pH range 4 to 10. Croce and colleagues (2015) used a wound 125 μm platinum (Pt) and silver wire to fabricate a coil-type electrochemical pH sensing device. They also devised a coil-type pH sensing device with a Ag/AgCl reference electrode, and a saturated calomel electrode (SCE), a Bluetooth transceiver and computer were used to record the data. Zhou and colleagues (2015) used an optical fiber sensor to measure the pH of solutions. The experimental data was transferred to a computer by Zigbee wireless network.

Given the existing body of research, this paper examines a wireless sensing system that uses an XBee module (Chou *et al*. 2016; Chou *et al*. 2018). The XBee wireless sensing system was used to detect sensitivities to many kinds of chemical substances and properties including: pH (following Chou *et al*. 2016), and glucose and lactate (Chou *et al*. 2018). The advantages of the XBee wireless sensing system are its high stability, low cost, portability, ease of operation, rapid detection and real-time monitoring functionality.

Cloete and colleagues (2016) successfully integrated flow, temperature, electrical conductivity and pH sensing properties of their device to both examine and record water quality data in real-time. Abouzar, Michelson, and Hamdi (2016) used a similar Zigbee system to investigate the sensing characteristics offered by wireless sensor networks in a precision agriculture setting.

In order to develop a real-time monitor for chloride ions, the XBee needs to be integrated with a flexible arrayed ruthenium dioxide (RuO_2)/ graphene oxide (GO) chloride ion sensor. Sensitivity, dynamic microfluidic measurements, hysteresis effects, selectivity coefficients and lifetime all affect calibration, as does the choice of using a RuO_2/GO chloride ion sensor. The wireless chloride sensing devices can be applied to detection of chloride ion concentrations in swimming pools or aquariums.

2. EXPERIMENTS

2.1 Ruthenium Dioxide Film

The Nernst's mathematical equation predicting the potential between the sensing and reference electrodes versus the pH value is given by formula (1) (Sardarinejad et al. 2015):

$$E = E^0 - 2.303 \frac{RT}{F} \text{ pH} = E^0 - 0.05916 \text{ pH} \quad (1)$$

Where E is the electromotive force (EMF), measured as the ion-selective electrode potential reduced external reference electrode potential, E^0 is the reference electrode potential, R is the gas constant, T is the absolute temperature and F is the Faraday constant. The RuO_2 membranes have low electrical resistivity, a high specific surface area, and high enzyme adhesion properties (Chou *et al*. 2014). Therefore, the RuO_2 thin film has excellent potential as a sensing material for hydrogen ion sensing devices.

2.2 Graphene Oxide

Figure 1 shows that GO contains the hydroxyl (OH) and carboxyl (COOH) groups. The protonation and de-protonation of the OH and COOH groups is accompanied by pH variations

(Kim, Hong, and Yang 2015; Melai *et al*. 2016; Salvo *et al*. 2018;). The specific surface area of the GO was larger than that of the reduced graphene oxide (rGO) and graphene. Lawal (2015) studied the preparation and characteristics of graphene for such purposes. The characteristics discovered were good conductivity and large surface area. The graphene could perform an "electron wire" on the redox centers of a protein, enzyme, or on the surface of an electrode, making it an exceptional substance for electrochemical biosensors. The GO membrane would thus serve as the chloride ion sensing film.

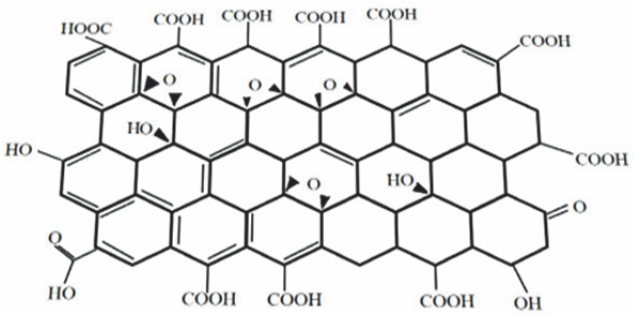

Fig. 1 GO structure (Salvo *et al.* 2018).

2.3 Sensing Theory of the Chloride Ion Sensing Film

The chloride ionophore III (ETH9033) and tridodecylmethy-lammonium chloride (TDDMACl) were fixed using polyvinyl chloride (PVC) as a polymer so that the adsorption force in the chloride atoms could strengthen the link. PVC, Dioctyl sebacate (DOS), chloride ionosphere III (ETH9033) and tridodecylmethy-lammonium chloride (TDDMACl) were used to prepare the chloride ion sensing film. DOS was used as a plasticizer, which softened the polymer member. The ETH9033 was used as an organic mercury ionophore. There were two mercury atom bases orthogonal to the benzene derivatives, and every mercury ionosphere was bonded to a chloride ion. The TDDMACl permitted transmission between the migrated anions and anions in the solution. The weight ratios of PVC : DOS : ETH9033 : TDDMACl were 33 : 66 : 2: 10 (wt%).

Compared to other chloride ion sensing electrodes, this sensor showed higher sensitivity. The chemical reaction process when exposed to chloride ions, followed Ar-Hg-R+X^- (Rothmaier *et al*. 1996), where Ar-Hg-R represents a mercury organic compound, and X is the chloride ion. The membranes with native compounds Ar-Hg-R appeared in reactions with aqueous solutions containing strong interfering substances, X^- (iodide, thiocyanate, or bromide), which caused a gradual replacement of substituents at the mercury centers. The Nersntian equation of the chloride sensing membrane is shown in formula (2) (Cheng *et al*. 2011), where E is the electromotive force (EMF) measured by the ion-selective electrode potential, minus the external reference electrode potential, E_0 is the initial voltage, α is the activity level of the ion, R is the gas constant 8.316 $mole^{-1}$ deg^{-1}, and F is the Faraday coefficient 96487 Coulomb.

$$E = E_0 - 2.303\frac{RT}{F}\log\alpha = E_0 - 0.05916\,pCl \qquad (2)$$

2.4 Fabrication of the Flexible Arrayed RuO_2/GO Chloride Sensor

Figure 2 shows a schematic diagram of the tested RuO_2/GO chloride sensor. The preparation method follows existing methods (Tseng *et al*. 2018; Chou *et al*. 2012), where 2 μL of chloride ion mixture was dropped onto the sensing windows of the RuO2/GO sensors. The RuO_2/GO sensor were dried at room temperature (25 °C) for 4 days. A photograph of the flexible arrayed RuO_2/GO chloride sensor is provided in Fig, 3. The dimensions of the flexible arrayed RuO_2/GO chloride sensor was 48 mm × 38 mm.

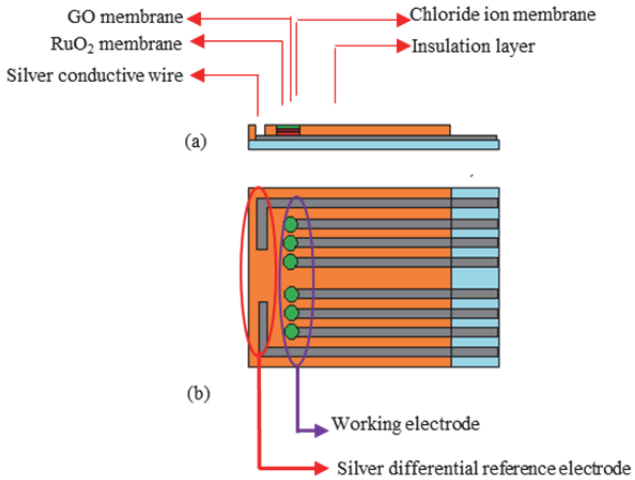

Fig. 2 Schematic diagram of the RuO_2/GO chloride sensor showing (a) the different sensing structures and, (b) locations of the working and silver differential reference electrode.

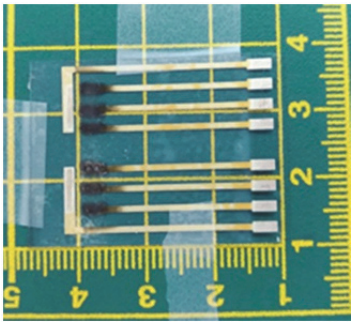

Fig. 3 Photograph of the RuO_2/GO flexible arrayed chloride sensor (48 mm × 38 mm).

2.5 Wireless Sensing System

An additional schematic diagram of the wireless sensing system including the XBee module is shown in Fig. 4. This is accompanied by a photograph of the wireless sensing system in Fig. 5. The XBee wireless sensing system is comprised of the XBee router, XBee coordinator, a computer (including LabVIEW 2012 software), a power supply, a 6-channel instrumentation amplifier (AD623), a circuit readout device, an Arduino Mega 2560, and the flexible arrayed RuO_2/GO chloride sensor. The sensing mechanism of tested sensor are shown in formula (3) and Fig. 6 (Chou *et al*. 2013). The sensing device included a differen-

tial Ag reference electrode, Ag contrast electrode and a chloride ion sensing electrode. The Ag reference electrode was connected to the ground loop, the Ag contrast electrode was linked to the positive electrode of the instrumentation amplifiers (AD623), and the bare silver reference electrodes were unlikely to be responsive to chloride ions. V_{Ref} was the response voltage of the Ag reference electrode, V_{Sen1} was the response voltage of the Ag contrast electrode, V_{Sen2} was the response voltage of the working electrode. V_{In1} was the voltage difference between the Ag contrast electrode and the reference electrode and V_{In2} was the voltage difference between the chloride sensing electrode and the Ag reference electrode. V_{Out} was the output voltage of AD623.

$$V_{Out} = V_{In1} - V_{In2} = (V_{Sen1} - V_{IRef}) - (V_{Sen2} - V_{IRef}) = V_{Sen1} - V_{Sen2} \quad (3)$$

The wireless sensing system described and shown in Fig 4 was used to measure response voltages from the sensor as it was subjected to different chloride ion concentrations in NaCl solutions, the solutions ranging between 10^{-5} M and 1 M. The sensitivity, selectivity coefficient and hysteresis voltage were all detected and recorded by the XBee system. Flow rates varied from 5 µL/min to 40 µL/min and Fig. 7 shows the wireless sensing system, microfluidic device and syringe pump used to measure the response voltages and real-time chloride ion levels.

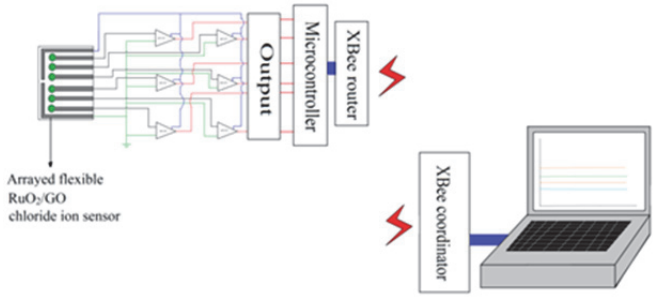

Fig. 4 Schematic diagram of the RuO_2/GO chloride sensor and wireless sensing system.

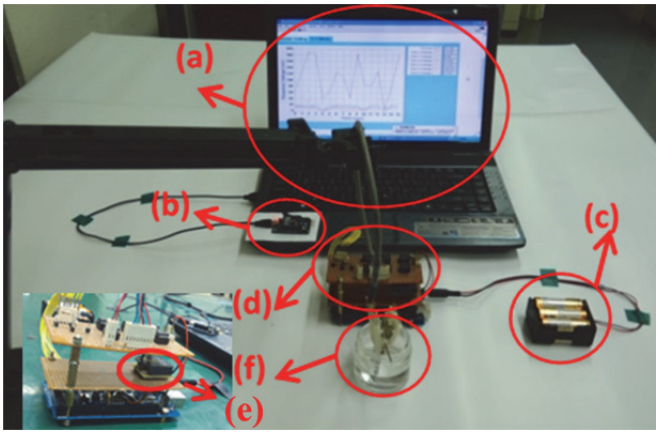

Fig. 5 Labelled photo of the flexible arrayed RuO_2/ GO chloride ion sensor and wireless sensing system (a) computer, (b) XBee coordinator, (c) power supply, (d) wireless sensor, (e) XBee router, and (f) the flexible arrayed RuO_2/GO chloride sensor.

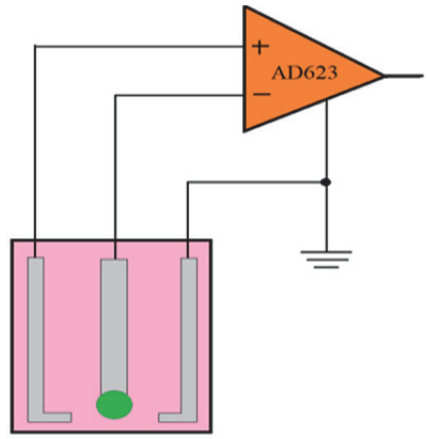

Fig. 6. Schematic diagram of the flexible arrayed RuO_2/GO chloride sensor and readout circuit (AD623).

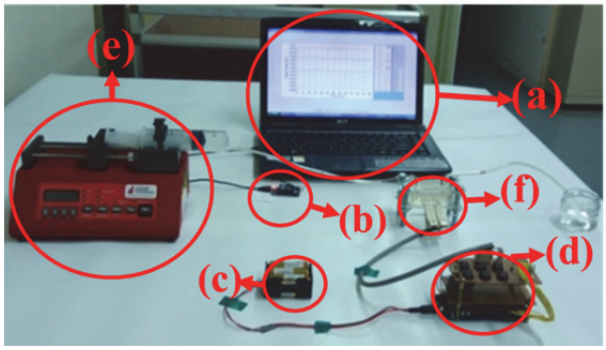

Fig. 7 Labelled photo of the microfluidic dynamic system with wireless functionality, (a) computer, (b) XBee coordinator, (c) power supply (d) XBee router, (e) syringe pump, and (f) microfluidic device.

3. RESULTS AND DISCUSSION

3.1 Sensing Characteristics under Static Solution

The sensitivity and linearity test results are shown in Fig. 8, where the average sensitivity and linearity were 47.84 mV/pCl and 0.99, respectively. Because the Arduino Mega 2560 was 10 bits, the resolution of the response voltage was greater than the sensitivity. The average sensitivity comparisons relative to similar devices in other literature are shown in Table 1. The wireless transmission protocols used were RFID (Zhou *et al*. 2017) and Bluetooth (Cheng *et al*. 2012). Zhou and colleagues (2017) tested a wireless chloride ion sensor that had an average sensitivity of 47.83 mV/pCl. This study used a voltage-time (V-T) measurement system to measure the response voltages, and derived sensitivity to chloride ions the same way (Chou *et al*. 2012; Tseng *et al*. 2018;). The detection distance of the V-T measurement system and chloride ion sensing device were less than when using the XBee wireless system. In order to calculate sensor detection limits, the response potentials absolute values were recorded and plotted, as shown in Fig. 5. According to the observed response potentials under different NaCl concentrations, an approximate straight line could be obtained by Origin 7.0. The estimate of the detection limit is given by extending the line to it's X intercept, which for this experiment was about 7×10^{-8} M.

Table 1 Comparative chloride ion sensing devices for different chloride ion concentrations.

Sensing electrode	Measurement system	Test solutons (M)	Average sensitivity (mV/pCl)	Ref.
RuO_2/0.01 wt% GO/Chloride ion selective membrane	XBee wireless V-T sensing system	10^{-5} to 1 NaCl solutions	47.84	This study
Ag/AgCl electrode and reference electrode	RFID communication protocol	10^{-4} to 1 NaCl solutions	47.8	(Zhuiykov, 2012)
ITO glass /SnO_2/ Chloride ion selective membrane	Bluetooth wireless measurement system	10^{-4} to 1 NaCl solutions	51.4	(Harris *et al.* 2016)
Silicon substrate/ RuO_2/ chloride ion selective membrane	Voltage-time (V-T) measurement system and wireless remote control platform	0 to 1.34×10^{-4} NaClO solutions	1.8 mV/ppm	(Nyni *et al.* 2017)
Silicon wafer /RuO_2/ chloride ion selective membrane	Current-voltage (I-V) measurement system with three Keithley 236 semiconductor parameter analyzers	10^{-4} to 1 NaCl solutions	59.0	(Cheng *et al.* 2012)
Polyethylene terephthalate /dupont 5876 AgCl conducting paste/ dupont 8153 insulating paste/ pHEMA hydrogel layer	High impedance voltmeter (Keithley 617A)	10^{-3} to 3 NaCl solutions	58.0	(Chou *et al.* 2012)
Polyethylene terephthalate /RuO_2/0.01 wt% GO/Chloride ion selective membrane	V-T measurement system	10^{-5} to 1 NaCl solutions	44.5	(Tseng *et al.* 2018)
Polyethylene terephthalate /RuO_2/Chloride ion selective membrane	V-T measurement system	10^{-4} to 1 NaCl solutions	26.2	(Chou *et al.* 2012)

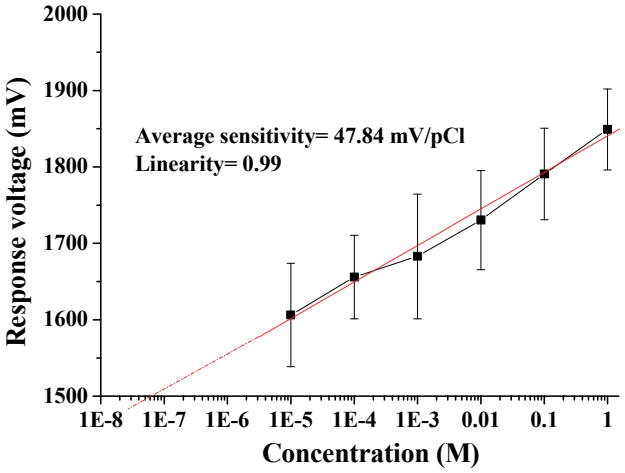

Fig. 8 Response voltage curve versus concentration for the flexible arrayed RuO_2/GO chloride ion sensor and integrated XBee wireless sensing system for 10^{-5} M and 1 M NaCl solutions.

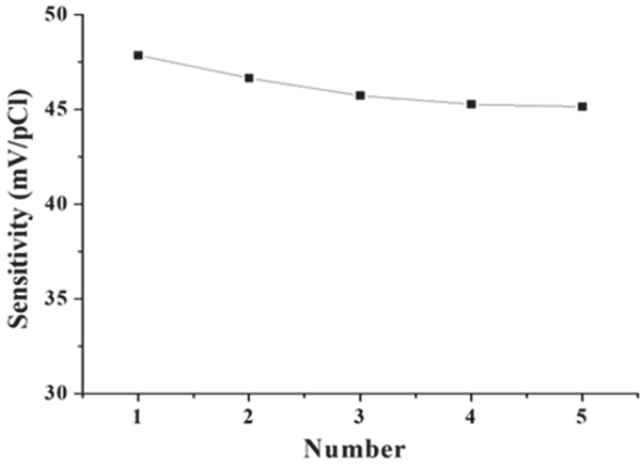

Fig. 9 Repeatability of the flexible arrayed RuO_2/GO chloride sensor.

The devised sensor was also tested for repeatability. Figure 9 shows the measurement of five repetitions of the experiment. Average sensitivities were between 45.13 mV/pCl and 48.74 mV/pCl.

3.2 Dynamic Microfluidic Sensing Characteristics

The sensitivity of the XBee wireless chloride ion sensor is shown in Fig. 10. Average sensitivity increased when the flow rates increased from 5 μL/min to 40 μL/min. A boundary layer was produced by friction and viscous force; the boundary layer was between the chloride membrane and the molecular electrolyte (Chou *et al*. 2012; Tseng *et al*. 2018).

Boundary layer thickness decreased as flow rate increased, causing the average sensitivity of the chloride sensor to increase as flow rates increased. The best average sensitivity and linearity recorded were 60.64 mV/pCl and 0.98 at 35 μL/min, respectively. When the flow rate was over 35 μL/min, the sensitivities decreased. The flexible arrayed RuO_2/GO chloride sensor with the XBee wireless sensing system displayed a quick response and was convenient to operate, meaning that it has potential for real-time medical use.

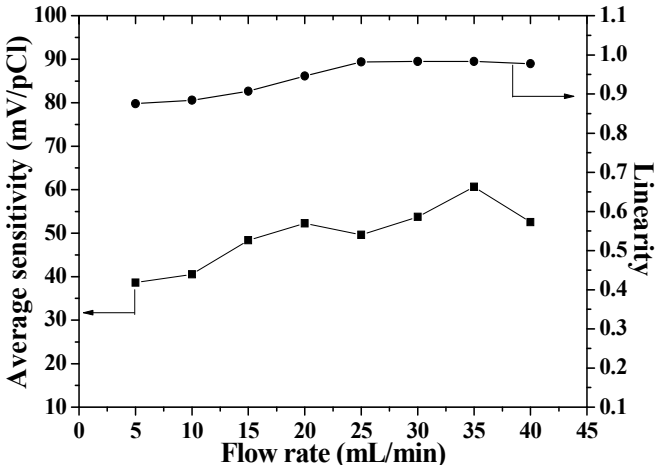

Fig. 10 Flexible arrayed RuO_2/GO chloride sensor with XBee wireless system, average sensitivity and linearity at flow rates between 5 µL/min and 40 µL/min.

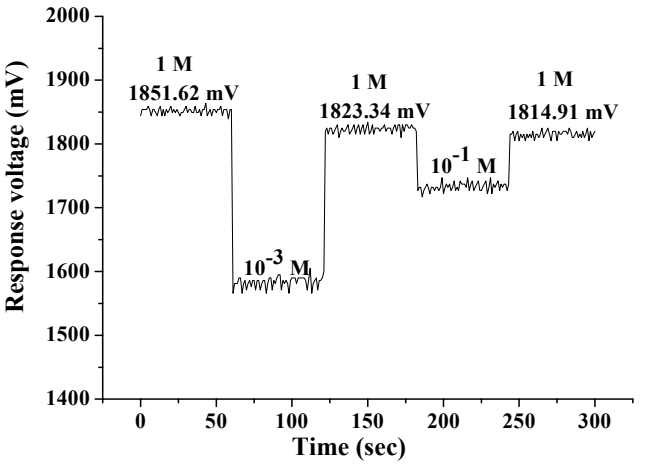

Fig. 12 Response voltages of the flexible arrayed RuO_2/GO chloride sensor in NaCl solutions for the cycle: 1 M → 10^{-3} M→ 1 M → 10^{-1} M → 1 M.

3.3 Investigation of the Hysteresis Voltage

In this study, the hysteresis voltage was defined by immersing the biosensor in the following cycle of concentrations: 1 M → 10^{-1} M → 1 M → 10^{-3} M → 1 M. The response voltages of the sensor were measured by a V-T system, with different cycles of chloride ion concentrations between 10^{-3} M and 1 M NaCl. The experimental results are shown in Fig. 11 and Fig. 12. Hysteresis voltages were 50.14 mV and 36.71 mV during the different solution cycles, where one solution cycle was 1 M → 10^{-1} M → 1 M → 10^{-3} M → 1 M and another was 1 M→ 10^{-3} M → 1 M → 10^{-1} M → 1 M.

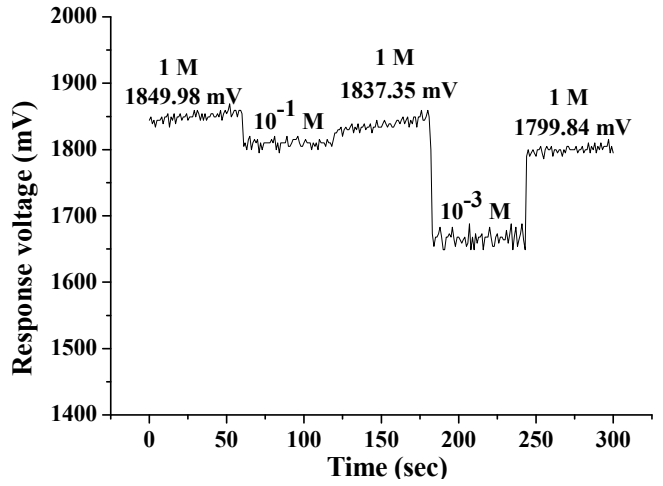

Fig. 11 Response voltages of the flexible arrayed RuO_2/ GO chloride sensor in NaCl solutions for the cycle: 1 M → 10^{-1} M → 1 M → 10^{-3} M → 1 M.

3.4 Lifetime

Re-usability of the wireless chloride sensing devices was tested. Figure 13 shows that sensitivity was 47.82 mV/pCl on the first day, but by day 7, sensitivity was 45.83 mV/pCl. By day 14, sensitivity was 43.56 mV/pCl, and at day 21, sensitivity was 37.47 mV/pCl. Testing continued until day 28, when sensitivity was 32.51 mV/pCl. When the sensors were not in use, they were kept refrigerated at 4 °C to maintain stability.

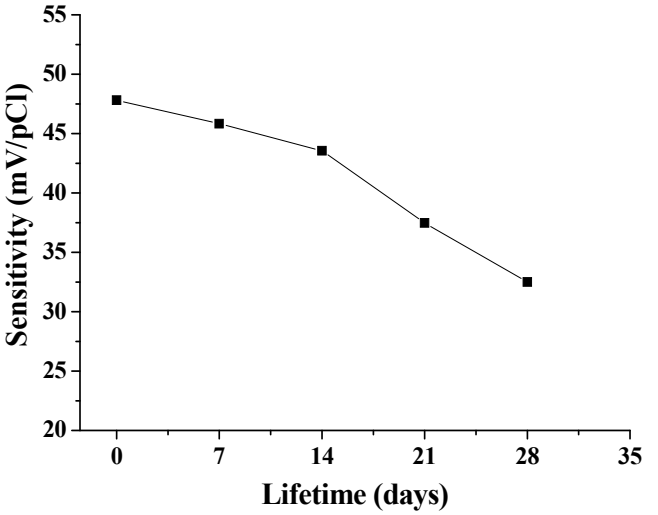

Fig. 13 Flexible arrayed RuO_2/GO chloride sensor with XBee wireless system, lifetime tests.

3.5 Chloride Ion Detection of Tap Water

Water chlorination at treatment plants is an important part of the process for producing potable water. Current sterilization capabilities come from free chloride that is derived from hypochlorous acid (HClO) and hypochlorite ions (ClO^-) (Helbling, and Briesen, 2008; Kumar, John, and Indira, 2006; Muñoz, Céspedes, and Baeza, 2015). The wireless sensing system tested here was used to investigate the sensitivity and linearity to different NaClO solutions ranging from 10^{-6} M to 1 M. Fig. 14 shows that the average sensitivity and linearity were 28.92 mV/pCl and 0.98, respectively, and that the sensor had good stability for detecting chloride concentrations. Figure 15 shows that the average response voltage was 1978.34 ± 9.89 mV in tap water as recorded by the XBee system. The chloride concentration ranges of the tap water were between 10-5 M and 10^{-4} M.

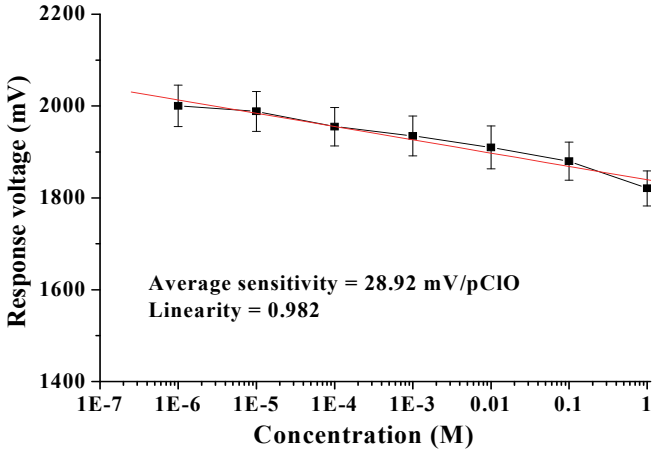

Fig. 14 Curve of response voltage versus concentration for the flexible arrayed RuO_2/GO chloride sensor with XBee wireless system in 10^{-6} M to 1 M NaClO solutions.

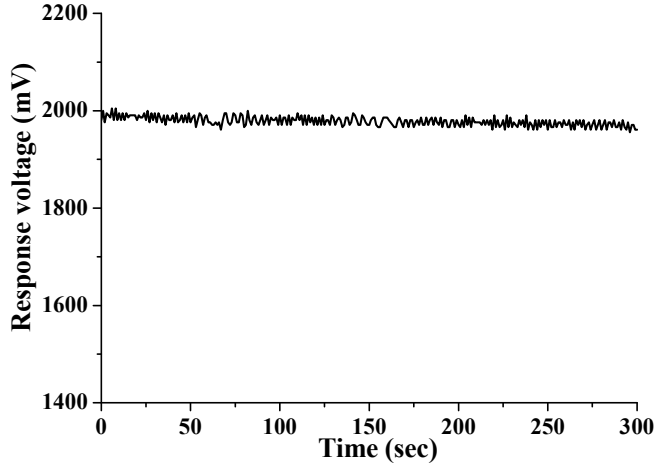

Fig. 15 Response voltage changes over time for the flexible arrayed RuO_2/GO chloride sensor with XBee wireless system in tap water.

4. CONCLUSION

Average sensitivity of the chloride sensor with XBee wireless system was 47.84 mV/pCl and linearity was 0.99. The average sensitivity of the flexible arrayed RuO_2/GO chloride sensor with XBee wireless system and dynamic microfluid was 60.64 mV/pCl and linearity was 0.98 at 35 μL/min. The hysteresis voltages were 50.14 mV and 36.71 mV during the different solution cycles. The solution cycle tested was 1 M → 10^{-1} M → 1 M → 10^{-3} M → 1 M, and the alternate cycle was 1 M → 10^{-3} M → 1 M → 10^{-1} M → 1 M. The selectivity coefficients of the ClO^- ion, ClO_4^- ion, NO_3^- ion and I^- ion with Cl^- ion were 5.0×10^{-2}, 1.0×10^{-1}, 5.9×10^{-3} and 5.6×10^{-1}, respectively. The above experimental results demonstrate that the tested wireless sensing system with the flexible arrayed RuO_2/GO chloride sensor has good selectivity and stability for chloride detection.

REFERENCES

Aisopou, A., Stoianov, I., and Graham, N.J.D. (2012). "In-pipe water quality monitoring in water supply systems under steady and unsteady state flow conditions: a quantitative assessment." *Water Res.*, **46**, 235-246.

Abbas, Y., Have, B.T., Hoekstra, G.I., Douma, A., Bruijn, D.D., Olthuis, W., and Berg, A.V.D. (2015). "Connecting to concrete: wireless monitoring of chloride ions in concrete structures." *Procedia Eng*, **120**, 965-968.

Abouzar, P., Michelson, D.G., and Hamdi, M. (2016). "RSSI-based distributed self-localization for wireless sensor networks used in precision agriculture." *IEEE Trans. Wireless Commun.*, **15**, 6638-6650.

Chou, J.C., Chen, J.T., Liao, Y.H., Lai, C.H., Chen, R.T., Tsai, Y.L., Lin, C.Y., Chen, J.S., Huang, M.S., and Chou, H.T. (2016). "Wireless sensing system for flexible arrayed potentiometric sensor based on XBee module." *IEEE Sens. J.*, **16**, 5588-5595.

Chou, J.C., Yan, S.J., Liao, Y.H., Lai, C.H., Wu, Y.X., and Wu, C.Y. (2018). "Remote detection for glucose and lactate based on flexible sensor array." *IEEE Sens. J.*, **18**, 3467-3474.

Cloete, N.A., Malekian, R., and Nair, L. (2016). "Design of smart sensors for real-time water quality monitoring." *IEEE Access*, **4**, 3975-3990.

Cheng, J.F., Chou, J.C., Sun, T.P., Hsiung, S.K., and Kao, H.L. (2012). "Study on a multi-ions sensing system for monitoring of blood electrolytes with wireless home-care system." *IEEE Sens. J.*, **12**, 967-977.

Chou, J.C., Chen, C.C., and Lee, C.C. (2012). "Development of microcontroller applied to chlorine ion measurement system." *IEEE Sens. J.*, **12**, 2215-2221.

Croce, R.A., Vaddiraju, S., Legassey, A., Zhu, K., Islam, S.K., Papadimitrakopoulos, F., and Jain, F.C. (2015). "A highly miniaturized low-power cmos-based pH monitoring platform." *IEEE Sens. J.*, **15**, 895-901.

Carbó, N., Carrero, J.L., Castillo, F.J.G., Tormos, I., Olivas, E., Folch, E., Fillol, M.A., and Soto, J. (2018). "Quantitative determination of spring water quality parameters via electronic tongue." *Sensors*, **18**, 1-12.

Cheng, J.F., Chou, J.C., Sun, T.P., Hsiung, S.K., and Kao, H.L. (2011). "Study on all-solid-state chloride sensor based on tin oxide/indium tin oxide glass." *Jpn. J. Appl. Phys.*, **50**, 037001-1–037001-8.

Chou, J.C., Tsai, Y.L., Cheng, T.Y., Liao, Y.H., Ye, G.C., and Yang, S.Y. (2014). "Fabrication of arrayed flexible screen-printed glucose biosensor based on microfluidic framework." *IEEE Sensors J.*, **14**, 178-183.

Chou, J.C., Ye, G.C., Wu, D.G., and Chen, C.C. (2012). "Fabrication of the array chlorine ion sensor based on microfluidic device framework." *Solid-State Electron.*, **77**, 87-92.

Chou, J.C., Wu, D.G., Tseng, S.C., Chen, C.C., and Ye, G.C. (2013). "Application of Microfluidic Device for Lactic Biosensor." *IEEE Sensors J.*, **13**, 1363-1370.

Dam, V.A.T., Zevenbergen, M.A.G., and Schaijk, R.van. (2016). "Toward wearable patch for sweat analysis." *Sens. Actuators, B*, **236**, 834-838.

Dang, W., Manjakkal, L., Navaraj, W.T., Lorenzelli, L., Vinciguerra, V., and Dahiya, R. (2018). "Stretchable wireless system for sweat pH monitoring." *Biosens. Bioelectron.*, **107**, 1092-202.

Gonski, S.F., Cai, W.J., Ullman, W.J., Joesoef, A., Main, C.R., Pettay, D. T., and Martz, T. R. (2018). "Assessment of the suitability of durafet-based sensors for pH measurement in dynamic estuarine environments." *Estuar. Coast. Mar. Sci.*, **200**, 152-168.

Harris, N., Cranny, A., Rivers, M., Smettem, K., and Lennard, E.G.B. (2016). "Application of distributed wireless chloride sensors to environmental monitoring: initial results." *IEEE Trans Instrum Meas*, **65**, 736-743.

Helbling, D.E. and Briesen, J.M.V. (2008). "Continuous monitoring of residual chlorine concentrations in response to controlled microbial intrusions in a laboratory-scale distribution system." *Water Res.*, **42**, 3162-3172.

Jung, J., Lee, J., Shin, S., and Kim, Y.T. (2017). "Development of a telemetric, miniaturized electrochemical amperometric analyzer." *Sensors*, **17**, 9 pages.

Kato, N., Hirano, N., Okazaki, S., Matsushita, S., and Gomei, T. (2017). "Development of an all-solid-state residual chlorine sensor for tap water quality monitoring." Sens. Actuators, B, **248**, 1037-1044.

Kim, T.Y., Hong, S.A., and Yang, S. (2015). "A solid-state thin-film Ag/AgCl reference electrode coated with graphene oxide and its use in pH sensor." *Sensors*, **15**, 6469-6482.

Kumar, K.G., John, K.S., and Indira, C.J. (2006). "A chloride ion-selective potentiometric sensor based on a polymeric schiff base complex." *Indian J. Chem. Technol*., **13**, 13-16.

Li, P., Zhang, D., Jiang, C., Zong, X., and Cao, Y. (2017). "Ultra-sensitive suspended atomically thin-layered black phosphorus mercury sensors." *Biosens. Bioelectron*., **98**, 68-75.

Li, P., Zhang, D.Z., Wu, J.F., Cao, Y.H., and Wu, Z.L. (2018). "Flexible integrated black phosphorus sensor arrays for high performance ion sensing." *Sens. Actuators*, *B*, **273**, 358-364.

Lu, L., Yan, G., Zhao, K., and Xu, F. (2015). "An implantable telemetry platform system with asic for in vivo monitoring of gastrointestinal physiological information." *IEEE Sens. J.*, **15**, 3524-3534.

Lawal, A.T. (2015). "Synthesis and utilization of graphene for fabrication of electrochemical sensors." *Talanta*, **131**, 424-443.

Melai, B., Salvo, P., Calisi, N., Moni, L., Bonini, A., Paoletti, C., Lomonaco, T., Mollica, V., Fuoco, R., and Francesco, F.D. (2016). "A graphene oxide pH sensor for wound monitoring." the 38th Annual International Conference of the IEEE Engineering in Medicine and Biology Society, EMBC 2016, Orlando, FL, USA.

Muñoz, J., Céspedes, F., and Baeza, M. (2015) "Modified multiwalled carbon nanotube/epoxy amperometric nanocomposite sensors with CuO nanoparticles for electrocatalytic detection of free chlorine." Microchem. J., **122**, 189-196.

Nyni, K.A., Vincent, L.K., Varghese, L., Liya, V.L., Johny, A.N., and Yesudas, C. V. (2017). "Wireless health monitoring system for ECG, EMG and EEG detecting." 2017 International Conference on Innovations in Information, Embedded and Communication Systems (ICIIECS), Coimbatore, India.

Ong, K.G., Paulose, M., and Grimes, C.A. (2003). "A wireless, passive, magnetically-soft harmonic sensor for monitoring sodium hypochlorite concentrations in water." *Sensors*, **3**, 11-18.

Rothmaier, M., Schaller, U., Morf, W.E., and Pretsch, E. (1996). "Response mechanism of anion-selective electrodes based on mercury organic compounds as ionophores." *Anal. Chim. Acta*, **327**, 17-28.

Rahimi, R., Brener, U., Chittiboyina, S., Soleimani, T., Detwiler, D.A., Lelièvre, S.A., and Ziaie, B. (2018). "Laser-enabled fabrication of flexible and transparent pH sensor with near-field communication for in-situ monitoring of wound infection." *Sens. Actuators*, *B*, **267**, 198-207.

Smettem, K., Klaus, J., Harris, N., and Pfister, L. (2017). "New potentiometric wireless chloride sensors provide high resolution information on chemical transport processes in streams." *Water*, **9**, 16 pages.

Sardarinejad, A., Maurya, D.K., Khaled, M., and Alameh, K. (2015). "Temperature effect on the performance of RuO_2 thin-film pH sensor." *Sens. Actuators*, *A*, **233**, 414-421.

Salvo, P., Melai, B., Calisi, N., Paoletti, C., Bllagambi, F., Kirchhain, A., Trivella, M.G., Fuoco, R., and Francesco, F.D. (2018). "Review paper: graphene-based devices for measuring pH." *Sens. Actuators*, *B*, **256**, 976-991.

Tseng, S.C., Wu, T.Y., Chou, J.C., Liao, Y.H., Lai, C.H., Chen, J.S., Yan, S.J., Huang, M.S., Tseng, T.W., and Nien, Y.H. (2018). "Research of Sensing Characteristic and Dynamic Measurement of Graphene Oxides Modified Flexible Arrayed RuO_2 Chlorine Ion Sensor." *Mater. Res. Bull.*, **101**, 155-161.

Yue, R. and Ying, T. (2012). "A novel water quality monitoring system based on solar power supply & wireless sensor network." *Procedia Environmental Sciences*, **12**, 265-272.

Zhuiykov, S. (2012) "Solid-state sensors monitoring parameters of water quality for the next generation of wireless sensor networks." *Sens. Actuators*, *B*, **161**, 1-20.

Zhou, S., Sheng, W., Deng, F., Wu, X., and Fu, Z. (2017). "A novel passive wireless sensing method for concrete chloride ion concentration monitoring." *Sensors*, **17**, 1-13.

Zhou, B., Yang, S., Sun, T., and Grattan, K.T.V. (2015). "A novel wireless mobile platform to locate and gather data from optical fiber sensors integrated into a WSN." *IEEE Sens. J.*, **15**, 3615 -3621.